Developmental changes of coupling between presynaptic Ca^{2+} channels and release sensors at BC-PC synapse

Jingjing Chen, Peter Jonas

Institute of Science and Technology Austria, Am Campus 1, A-3400 Klosterneuburg, Austria

Introduction

The coupling between Ca^{2+} channels and Ca^{2+} sensors of exocytosis is a key factor that determines the speed and efficacy of synaptic transmission. Previous work revealed that different synapses rely on different coupling configurations. GABAergic synapses often show “nanodomain” coupling, with a coupling distance between Ca^{2+} channels and release sensors of 10–20 nm. Nanodomain coupling conveys several functional advantages, including speed and efficiency of synaptic transmission. In contrast, various glutamatergic synapses rely on “microdomain” coupling, with a coupling distance of > 50 nm. Microdomain coupling may also offer advantages, including regulation of release probability during presynaptic plasticity.

In both microdomain and nanodomain coupling regimes, the exact coupling topography is largely unknown. Different scenarios have been be proposed, including random distribution of Ca^{2+} channels and vesicles, random distribution of Ca^{2+} channel clusters and vesicles, Ca^{2+} channels surrounding vesicles, and vesicles surrounding Ca^{2+} channel clusters. Recently, the coupling topology has been analyzed using a combination of electrophysiological analysis and FRL at the calyx of Held and cerebellar parallel fiber synapses. At these synapses, the results were consistent with a “perimeter” or an “exclusion zone” model, but less so with a “supercluster” model. Whether this is a general principle that applies to both nanodomain and microdomain coupling is, however, unclear.

The coupling configuration in presynaptic terminals is not static, but is regulated during developmental maturation of the synapse. At both the calyx of Held and cerebellar parallel fiber synapses, coupling becomes significantly tighter during development, implying a switch from microdomain to nanodomain coupling. During maturation, both the number of presynaptic Ca^{2+} channels and the number of docked vesicles per active zone decreases. The ratio of Ca^{2+} channel clusters to docked synaptic vesicles is close to 1, and tightly regulated during development. Whether these rules apply generally to other types of synapses is, however, unclear.

The cerebellar basket cell (BC)–Purkinje cell (PC) synapse shows a particularly tight coupling between Ca^{2+} channels and release sensors. At these synapses, the coupling distance between source and sensor probed with Ca^{2+} chelators is only 10–14 nm, which is in the range of direct molecular interactions. This raises the intriguing question of how the exact quantitative coupling topography looks like at this synapse. Furthermore, the previous findings raise the question of whether the nanodomain coupling configuration is established early in development, or whether it emerges from microdomain coupling in the process of synaptic maturation. To address these questions, we combined paired recordings between synaptically connected neurons with FRL analysis of presynaptic Ca^{2+} channels in BC terminals.

Experimental methods

Cerebellar slice preparation

Parasagittal 250-mm-thick cerebellar slices from the vermis region were cut using a custom-built or a VT1200 vibratome. After decapitation, the brain was rapidly dissected out and immersed in ice-cold slicing solution containing: 87 mM NaCl, 25 mM $NaHCO_3$, 2.5 mM KCl, 1.25 mM NaH_2PO_4, 10 mM D-glucose, 75 mM sucrose, 0.5 mM $CaCl_2$, and 7 mM $MgCl_2$ (pH 7.4 in 95% O2/5% CO2, 325 mOsm). After 20-min incubation at 35 ℃, the slices were stored at room temperature. Slices were used for maximally 5 hr after dissection. Experiments were performed at 21-24 ℃.

Paired recording

During experiments, slices were superfused with a physiological extracellular solution containing: 125 mM NaCl, 2.5 mM KCl, 25 mM $NaHCO_3$, 1.25 mM NaH_2PO_4, 25 mM D-glucose, 2 mM $CaCl_2$, and 1 mM $MgCl_2$ (pH 7.4 in 95% O2/5% CO2, 325 mOsm). Intracellular solution used for the presynaptic BCs contained: 125 mM K-gluconate, 20 mM KCl, 0.1 mM EGTA, 10 mM phosphocreatine, 2 mM $MgCl_2$, 2 mM ATP, 0.4 mM GTP, 10 mM HEPES (pH adjusted to 7.28 with KOH, 310 mOsm); 0.2% biocytin was added in a subset of recordings. The presynaptic pipette resistance was 8–15 MΩ. BCs were recorded under current-clamp conditions. A holding current of approximately 50 pA was injected to maintain the membrane potential at approximately 65 mV and to avoid spontaneous AP generation. To evoke presynaptic APs, single pulses or trains of either ten pulses at 50 Hz or 50 pulses at 100 Hz (400 pA, 4 ms) were injected into the presynaptic BC every 4 or 20 s, respectively. PCs were recorded in the voltage-clamp configuration with a holding potential of 70 mV. For monitoring series and input resistance, 5-mV, 100-ms hyperpolarizing test pulses were applied after the IPSCs had decayed to baseline.

Data acquisition and analysis

Data were acquired with a Multiclamp 700B amplifier (Axon Instruments), low pass filtered at 10 kHz, and sampled at 20 or 50 kHz using a CED power1401 interface (Cambridge Electronic Design). Stimulus generation and data acquisition were performed using custom-made software (FPulse v3.33) running under Igor Pro 6.22 (WaveMetrics). Data were analyzed using Stimfit 0.14.9.

1 Connection between the BC-PC synapse

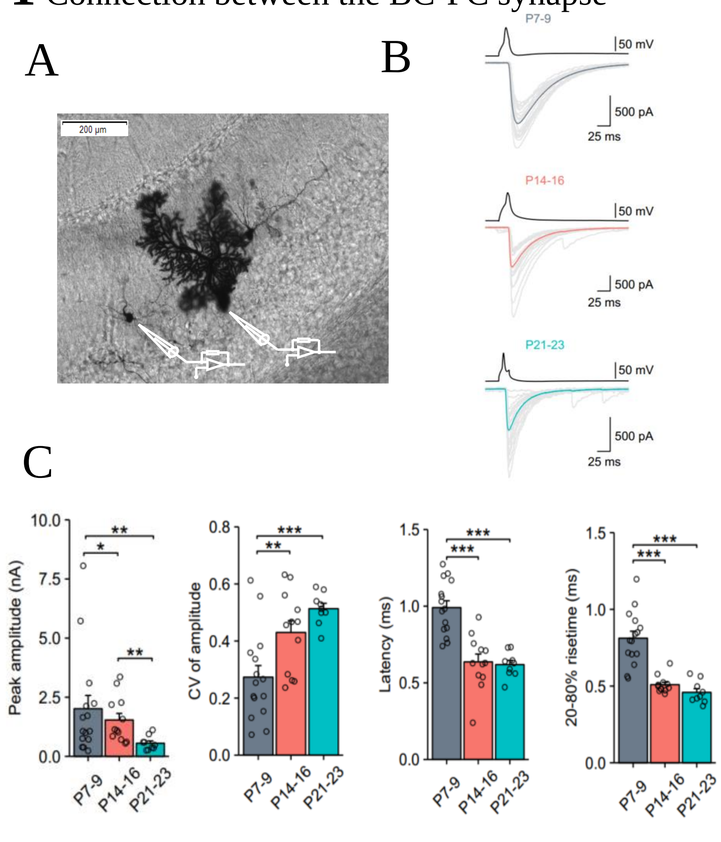

(A) Biocytin labeled basket cell (BC) and purkinjec cell (PC).
(B) Presynaptic evoked action potentials (grey) and evoked inhibitory postsynaptic currents (IPSCs) at P7-9, P14-16 and P21-23 respectively. 10 consecutive traces (light grey) and the average trace are show superimposed.
(C) Comparison of peak amplitude, CV of peak amplitude, lantency, and 20-80% rise time of evoked IPSCs.

2 Short term plasticity between the BC-PC synapse

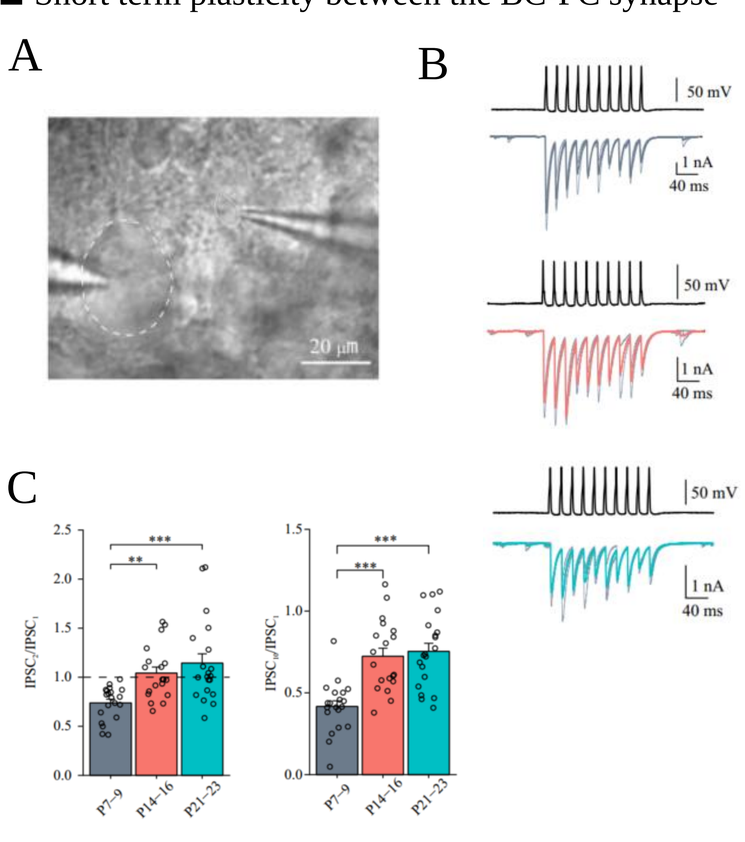

(A) Differential interference contrast optics and infrared light transmission (DIC-IR) images for patch-clamp recordingof BC-PC.
(B) Trains of 10 presynaptic action potentials evoked at 50 Hz (black) and corresponding IPSCs recorded from P7-9, P14-16 and P21-23 respectively. 10 consecutive traces (light grey) and averaged trace are shown superimposed.
(C) Plot of $IPSC_2/IPSC_1$ and $IPSC_{10}/IPSC_1$.

3 Types of Ca^{2+} channels in developing BC-PC synapse

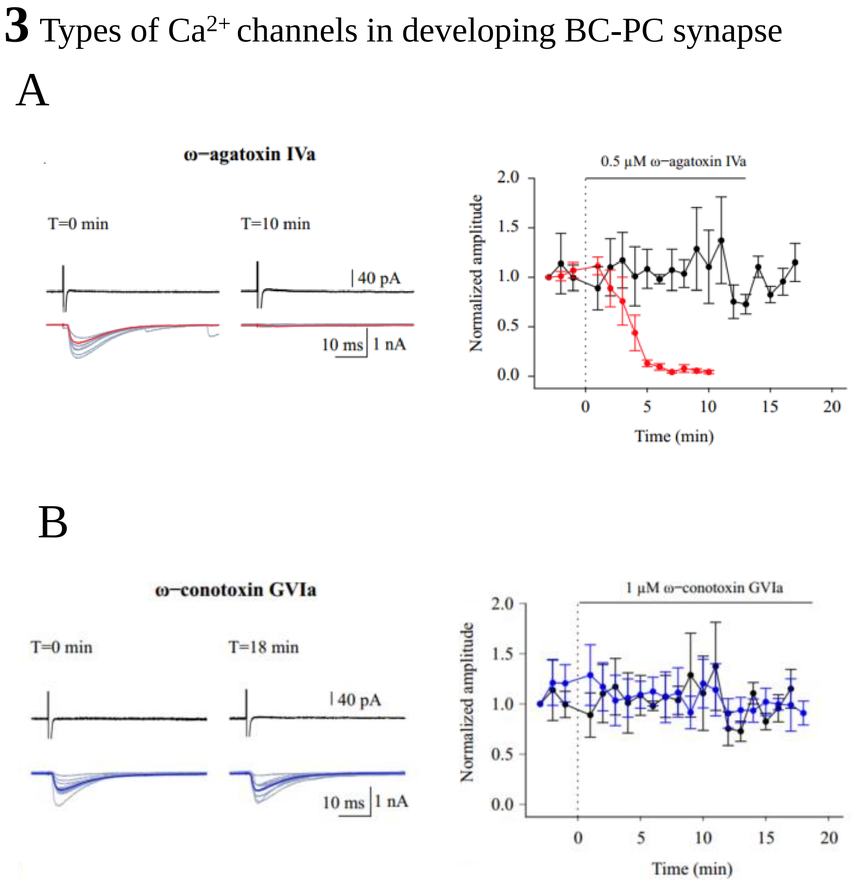

(A) Plot of IPSC peak amplitude against time during application of 0.5 µM ω-agatoxin IVα.
(B) Plot of IPSC peak amplitude against time during application of 1 µM ω-conotoxin GIVA

4 Quantal analysis of synaptic parameters during synaptic development.

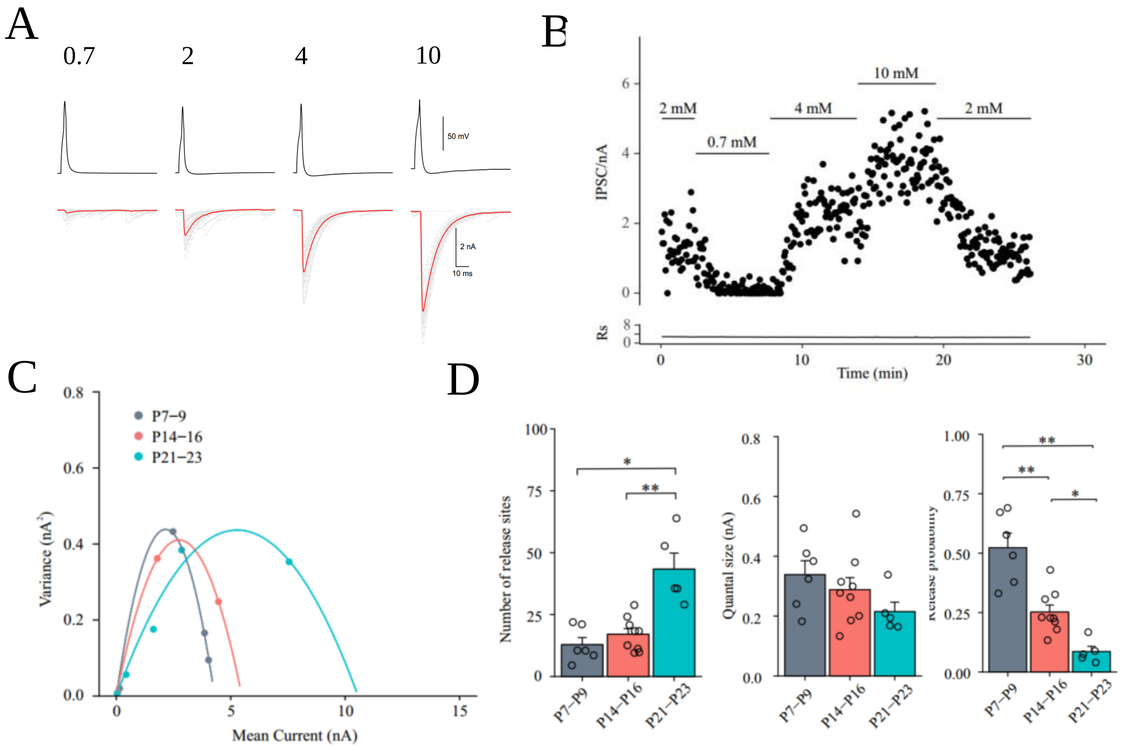

(A) Presynaptic action potentials (grey) and corresponding IPSCs in different $[Ca^{2+}]_o$ recorded from P14-16. 10 consecutive traces (light grey) and averaged trace are shown superimposed.
(B) Plot of IPSC peak amplitude against time during application of extracellular solutions with different $[Ca^{2+}]_o$.
(C) Variance and mean analysis of IPSC peak amplitude at different $[Ca^{2+}]_o$
(D) Histogram of number of release sites, release probability (Pr) and quantal size.

5 Synaptic development promotes facilitation and vesicle pool replenishment during stimulus trains at BC-PC Synapses

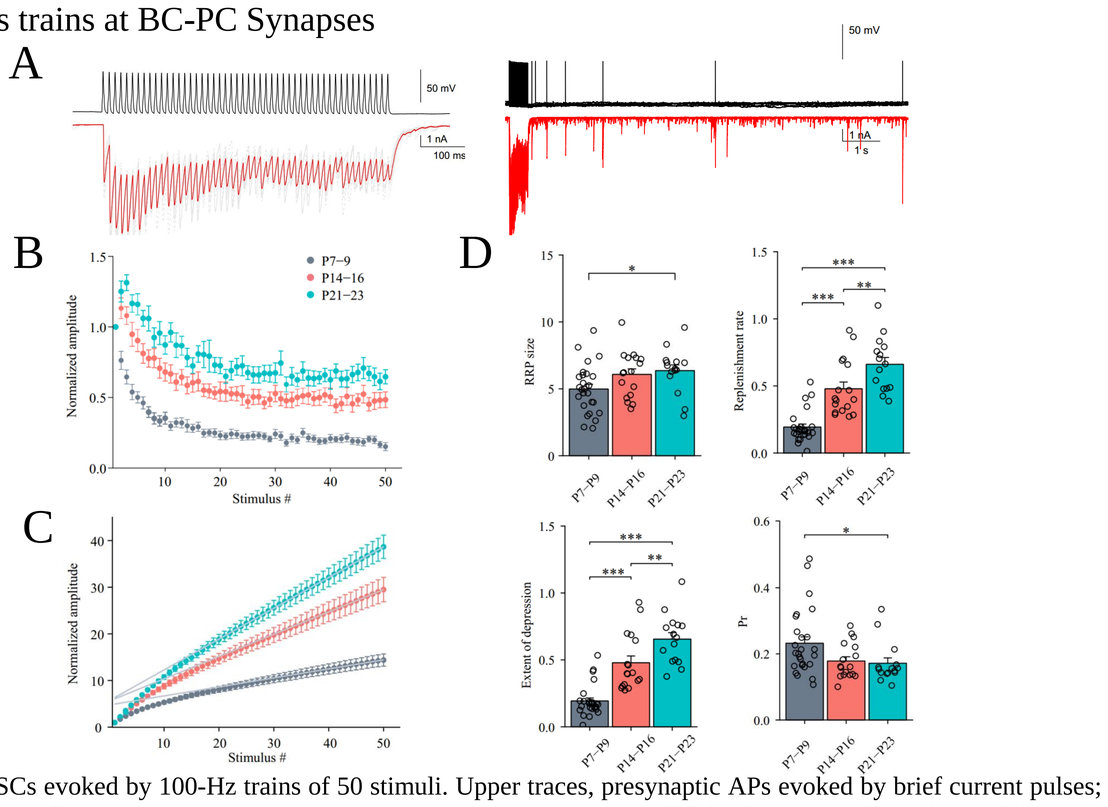

(A) Left: IPSCs evoked by 100-Hz trains of 50 stimuli. Upper traces, presynaptic APs evoked by brief current pulses; lower traces, IPSCs (gray traces, individual sweeps; red traces, average IPSCs) Right: 100-Hz trains of 50 stimuli followed by single test stimuli at variable time intervals. Overlay of 7 traces.
(B) Normalized IPSC peak amplitudes ($IPSCn/IPSC_1$) plotted against stimulus number (n).
(C and D) Quantitative analysis of pool size and refilling rate. IPSC peak amplitude was divided by $IPSC_1$, averaged across cells, and cumulatively plotted against stimulus number. The last ten points were fit by linear regression. Size of the readily releasable pool (RRP) was determined from intersection of the regression line with the ordinate, whereas refilling rate was determined from the slope of the line. Pr was quantified as the ratio of $IPSC_1$ over pool size. The extent of repression is calculated as the ratio of $IPSC_{50}/IPSC_1$.